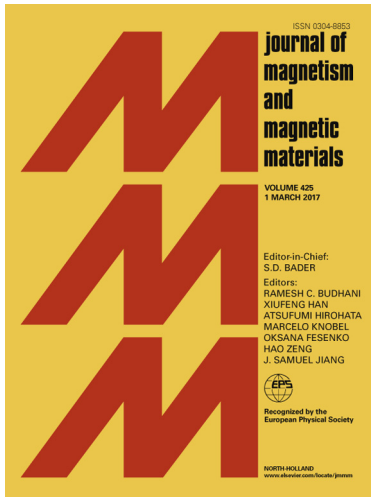

Research articles

Magnetization reversal of thin ferromagnetic elements with surface anisotropy

N.A. Usov, O.N. Serebryakova

PII: S0304-8853(17)32945-1
DOI: https://doi.org/10.1016/j.jmmm.2018.01.009
Reference: MAGMA 63587

To appear in: *Journal of Magnetism and Magnetic Materials*

Received Date: 19 September 2017
Revised Date: 20 December 2017
Accepted Date: 3 January 2018

Please cite this article as: N.A. Usov, O.N. Serebryakova, Magnetization reversal of thin ferromagnetic elements with surface anisotropy, *Journal of Magnetism and Magnetic Materials* (2018), doi: https://doi.org/10.1016/j.jmmm.2018.01.009

Magnetization reversal of thin ferromagnetic elements with surface anisotropy

N. A. Usov[1,2], O.N. Serebryakova[1,2]

[1]National University of Science and Technology «MISIS», 119049, Moscow, Russia

[2]Pushkov Institute of Terrestrial Magnetism, Ionosphere and Radio Wave Propagation, Russian Academy of Sciences, IZMIRAN, 108480, Troitsk, Moscow, Russia

Highlights

- Perpendicular and in-plane hysteresis loops of thin-film elements with surface anisotropy are calculated numerically.
- Buckling nucleation mode determines the nucleation field of elongated thin-film element.
- The nucleation field is proportional to the absolute value of the surface anisotropy constant.
- It is also inversely proportional to the element thickness.

Abstract. The magnetization reversal process in thin-film ferromagnetic elements with surface anisotropy of various shapes and sizes is investigated by means of numerical simulation. The dependencies of the perpendicular and in-plane hysteresis loops on the element thickness, and the value of the surface anisotropy constant are obtained. For sufficiently large values of the surface anisotropy constant the magnetization reversal of thin-film elements is shown to occur due to the nucleation of the buckling mode. For an elongated rectangular element the nucleation field of the buckling mode is proportional to the absolute value of the surface anisotropy constant, and inversely proportional to the element thickness.

Prime Novelty Statement

It is shown that analyzing the magnetization reversal process in thin-film ferromagnetic elements with surface anisotropy one can determine the actual value of the surface magnetic anisotropy by means of comparison of experimental and numerical simulation data. The properties of thin ferromagnetic films with surface anisotropy are promising for applications of such magnetic materials in modern thin-film electronics devices.

PACS: 75.50.Kj, 75.80.+q, 75.60.Ej, 75.60.Jk

Keywords: Thin ferromagnetic elements, Surface magnetic anisotropy, Buckling nucleation mode, Numerical simulation

Corresponding author: usov@obninsk.ru (N.A. Usov)

Introduction

The properties of thin ferromagnetic films with surface anisotropy are promising for applications of such magnetic materials in modern thin-film electronics devices [1-4]. From phenomenological point of view, the effect of surface anisotropy on the magnetization distribution in a ferromagnet can be described by introducing a special energy contribution to the total sample energy. The latter depends on the orientation of the unit magnetization vector $\boldsymbol{\alpha}(\boldsymbol{r})$ at the sample surface. Taking into account symmetry considerations, the energy density of the surface magnetic anisotropy in a simplest case can be written in the form [5-8]

$$w_{sa} = K_s(\vec{\alpha}\vec{n})^2, \qquad (1)$$

where K_s is the surface anisotropy constant, $\boldsymbol{n}$ being the unit vector perpendicular to the sample surface. If surface magnetic anisotropy constant K_s is negative and large enough in absolute value, a reorientation of the unit magnetization vector perpendicular to the film surface is energetically favorable, in spite of the increase in the magnetostatic energy of the ferromagnetic sample. The reorientation of the unit magnetization vector with a change in the ferromagnetic film thickness was observed in the number of experiments with thin films of iron, cobalt, and other ferromagnets [9-12].

Currently, it is supposed that the surface magnetic anisotropy can have various origins. It can be related with the specifics of the spin-orbit interaction on the sample surface [13], with the difference in the atomic lattices periods of the sample and substrate [14], with the distribution of inhomogeneous mechanical stresses near the interface [15], etc. However, from the point of view of the Micromagnetics [5] it is important that the energy contribution, Eq. (1), is concentrated in a very narrow region near the sample surface. Thus, it is a surface contribution to the total sample energy. As a result, its effect on the distribution of the unit magnetization vector in the volume of the ferromagnet can be properly described by the corresponding boundary condition acting on the sample surface.

This general approach has recently been consistently carried out [16] to study the equilibrium magnetization distributions in a thin ferromagnetic film with surface anisotropy by means of numerical simulation. It was shown [16] that if the magnitude of surface anisotropy constant K_s is less than a certain critical value, then there exists the so-called spin canted micromagnetic state in the intermediate range of film thicknesses, $L_{z,min} < L_z < L_{z,max}$, with average magnetization inclined at some angle to the sample surface. For sufficiently small thicknesses, $L_z < L_{z,min}$,, the film is magnetized perpendicular to the surface (z-state), while for $L_z > L_{z,max}$, the magnetization lies in the film plane. On the other hand, if the surface anisotropy constant exceeds the critical value, different labyrinth domain structures are realized [16] near the surface of the film of sufficiently large thickness.

In this paper the magnetization reversal process in thin-film ferromagnetic elements with surface anisotropy is studied by means of numerical simulation. Both in-plain and out of plane quasi-

static hysteresis loops of thin film elements of various shapes, thickness and in-plane dimensions are calculated. By comparison with the experimental data, the numerical results obtained would allow one to determine the value of the surface anisotropy constant of thin ferromagnetic film under investigation.

Numerical simulation

The numerical simulation is carried out for thin ferromagnetic nano elements of thicknesses L_z = 4 - 6 nm. We consider samples of circular and rectangular shape with different in-plane aspect ratios, L_x/L_y = 1.0 - 3.0, the in-plane dimensions of the elements being of the order of 100 - 400 nm. The elements are assumed to be cut out of a thin amorphous ferromagnetic CoSiB film [1, 2], with surface anisotropy, and with induced volume magnetic anisotropy in the plane of the film. The saturation magnetization of the CoSiB film is given by M_s = 500 emu/cm^3, the exchange constant $C = 2\times10^{-6}$ erg/cm, the anisotropy constant of the induced volume anisotropy is assumed to be $K_V = 10^4$ erg/cm^3. In the calculations performed the surface anisotropy constant varies within the range K_s = - (0.6 - 1.2) erg/cm^2.

For simplicity, it is further assumed that the surface anisotropy is present only at the upper boundary of the film. In this case, the micromagnetic boundary condition for the unit magnetization vector at $z = L_z$ has the form [5]

$$C\frac{\partial\alpha_x}{\partial z} = -2|K_s|\alpha_z^2\alpha_x; \qquad C\frac{\partial\alpha_y}{\partial z} = -2|K_s|\alpha_z^2\alpha_y; \qquad C\frac{\partial\alpha_z}{\partial z} = -2|K_s|\alpha_z\left(\alpha_z^2 - 1\right). \quad (2)$$

The usual boundary condition, $\partial\vec{\alpha}/\partial n = 0$, acts on other surfaces of the film.

The magnetization reversal process in thin-film elements with surface anisotropy is studied by solving the Landau-Lifshitz-Gilbert equation

$$\frac{\partial\vec{\alpha}}{\partial t} = -\gamma\left[\vec{\alpha}, \vec{H}_{ef}\right] + \kappa\left[\vec{\alpha}, \frac{\partial\vec{\alpha}}{\partial t}\right], \quad (3)$$

where γ is the gyromagnetic ratio, and κ is the phenomenological damping constant. The total effective magnetic field in the volume of the film takes into account the exchange, anisotropic, and magneto-dipole interactions

$$\vec{H}_{ef} = \frac{C}{M_s}\Delta\vec{\alpha} + \vec{H}_0 + \vec{H}' - \frac{\partial w_a}{M_s\partial\vec{\alpha}}. \quad (4)$$

Here $\vec{H}_0$ is the external applied magnetic field, $\vec{H}'$ is the demagnetizing field, $w_a = K_V\left(\alpha_y^2 + \alpha_z^2\right)$ is the energy density of the induced magnetic anisotropy with the easy anisotropy axis lying in the plane of the film and oriented along the *x* axis.

For numerical simulation the ferromagnetic film is approximated by small cubic numerical cells with an edge b = 1.5-3 nm, sufficiently small in comparison with the exchange length of the ferromagnet, $L_{ex} = \sqrt{C}/M_s \approx 28$ nm. In the calculations performed the thin-film elements were approximated by a sufficiently large number of numerical cells, $N \sim 10^5$, in order to maintain an accuracy of the numerical results obtained. To approximate numerically the boundary condition, Eq. (2), at the sample surface, the usual numerical method is to introduce additional auxiliary layer of the numerical cells outside the sample surface.

The calculation of the quasi-static hysteresis loop of a thin film element begins with the calculation of a quasi-homogeneous micromagnetic configuration in a sufficiently strong external magnetic field applied in-plane, or perpendicular to the film plane, respectively. Then, the external magnetic field decreases by a small value, dH_0 = 1 - 2 Oe, and the evolution of the unit magnetization vector $\boldsymbol{\alpha}(\boldsymbol{r})$ is calculated in accordance with Eqs. (2) - (4), until a new equilibrium micromagnetic state is reached. The magnetization distribution in applied magnetic field is considered to be stable when the criterion

$$\max_{(1\le i\le N)}\left|\left[\vec{\alpha}_i, \vec{H}_{ef,i}\middle/\left\|\vec{H}_{ef,i}\right\|\right]\right| < 10^{-6} \qquad (5)$$

is fulfilled. This means that the maximum deviation of the unit magnetization vector from the direction of the effective magnetic field in the same numerical cell does not exceed a small predefined value.

Results and discussion

In-plane hysteresis loops

Fig. 1 shows the in-plane quasi-static hysteresis loops of rectangular thin-film elements with different aspect ratios calculated numerically for various values of the surface anisotropy constant. The numerical cell size in these calculations is given by b = 3.0 nm. The decrease of the numerical cell size up to b = 1.5 nm does not change the numerical results obtained more than by 1-3%. One can see that the remanent magnetization of the elements studied decreases with increasing of the absolute value of the surface anisotropy constant. Moreover, the larger the absolute value of this constant, the greater the magnetic saturation field of the element. In addition, with an increase in $|K_s|$ the area of the hysteresis loop decreases substantially. The existence of in-plane remanent magnetization for the hysteresis loops 1)-3) in Fig. 1 corresponds to the spin canted magnetization state. The remanent magnetization is zero for perpendicular magnetized *z*-state. This case is exemplified by the curve 4) in Fig. 1b. In principle, such behavior of the hysteresis loops is expected, since the presence of surface anisotropy with $K_s < 0$

promotes the deviation of the unit magnetization vector perpendicular to the film plane, while the external magnetic field tries to orient the magnetization vector along the film surface.

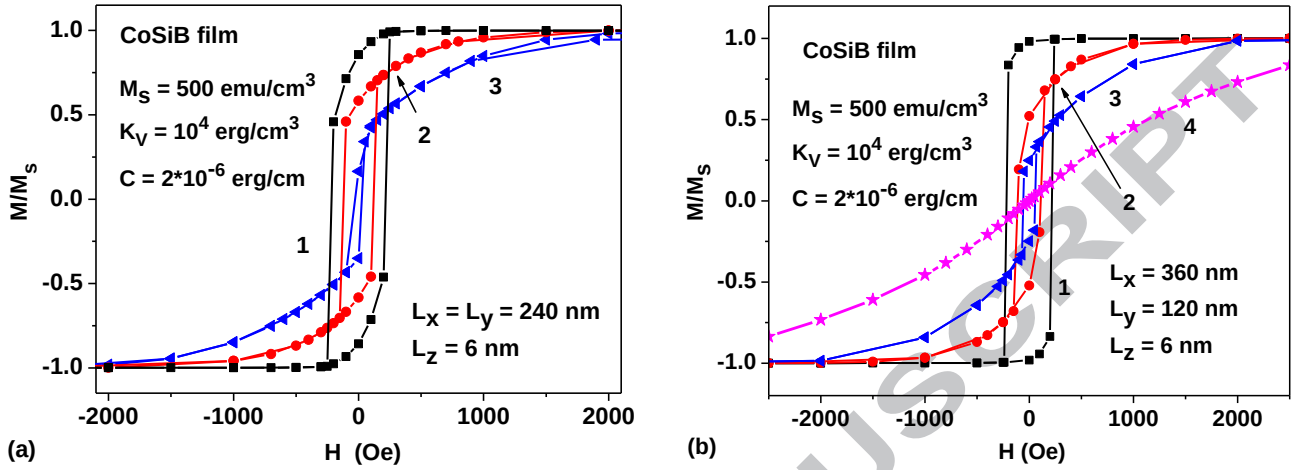

Fig. 1 Quasistatic hysteresis loops of rectangular CoSiB elements with different aspect ratios: a) L_x/L_y = 1.0; b) L_x/L_y = 3.0. The magnetic field is applied in the plane of the elements along the *x* axis. The calculations are carried out for different values of the surface anisotropy constant: K_s = - 0.7 erg/cm^2; 2) K_s = - 0.9 erg/cm^2; 3) K_s = - 1.0 erg/cm^2; 4) K_s = - 1.25 erg/cm^2.

In general, the calculation of the in-plane hysteresis loop for a thin-film element with surface anisotropy can be performed only by numerical simulation. At the same time, in the case of a perpendicularly magnetized z-state, the magnetization curve of a thin ferromagnetic film in a magnetic field H_0 applied along the film surface can be calculated analytically. Assuming the uniform rotation of the unit magnetization vector in this case, the total energy of the film per unit area can be written as [16]

$$w = \left(K_{ef} L_z - |K_s|\right)\cos^2\theta - M_s H_0 L_z \sin\theta, \qquad (6)$$

where $K_{ef} = K_V + 2\pi M_s^2$, θ is the angle of the unit magnetization vector with respect to the *z* axis.

Minimizing Eq. (6) as a function of θ, one obtains the equilibrium value of the *x*-component of the unit magnetization vector as a function of the applied magnetic field H_0

$$\alpha_x = \sin\theta = \begin{cases} H_0/H_s, & H_0 \le H_s \\ 1, & H_0 > H_s \end{cases}, \qquad (7)$$

where $H_s = 2\left(|K_s|/L_z - K_{ef}\right)/M_s$ is the corresponding saturation field of the film.

As an example, Fig. 2 shows the magnetization curves of perpendicular magnetized *z*-state in a thin-film element with thickness L_z = 4 nm calculated numerically (dots) for different values of the

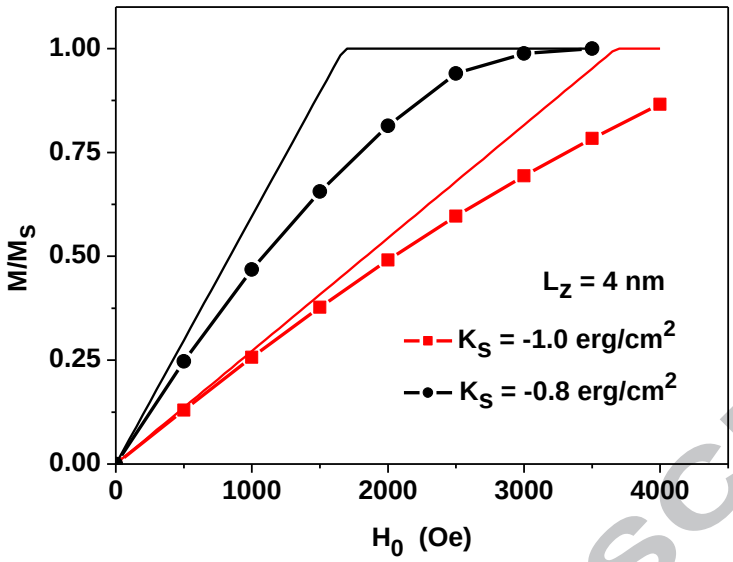

Fig. 2. Magnetization curves (dots) of the perpendicular magnetized z-state in rectangular element with thickness L_z = 4 nm and in-plane sizes L_x = 240 nm, L_y = 80 nm as the function of in-plane magnetic field for various values of the surface anisotropy constant. The solid lines are drawn in accordance with Eq. (7).

surface anisotropy constant. The numerical cell size in these calculations is given by b = 2 nm. The solid curves in Fig. 2 are drawn according Eq. (7). Some deviation of numerical results from Eq. (7) is explained by the influence of the demagnetizing field of the element of finite in-plane size. The in-plane demagnetizing field is created by magnetic charges that arise at the side ends of the element under the influence of in-plane magnetic field. This effect is not taken into account in Eqs. (6) and (7), which are valid for an infinite film. At the same time, as can be seen from Fig. 2, the slope of the magnetization curves in small magnetic fields is in satisfactory agreement with Eq. (7).

Perpendicular hysteresis loops

Let us now consider the magnetization reversal process in a thin-film element in magnetic field applied perpendicular to the film plane. In this case, the study of the magnetization reversal of the *z*-state is of the greatest interest, since the numerical results obtained can be compared with the analytical theory of the nucleation fields [5]. It is well known [5], that the magnetization reversal of a homogeneously magnetized ferromagnetic sample is initiated in a reversed applied magnetic field, which is called the nucleation field. The value of the nucleation field and the mode of the magnetization reversal can depend on various factors, in particular, on the shape, size and in-plane aspect ratio L_x/L_y of a rectangular element.

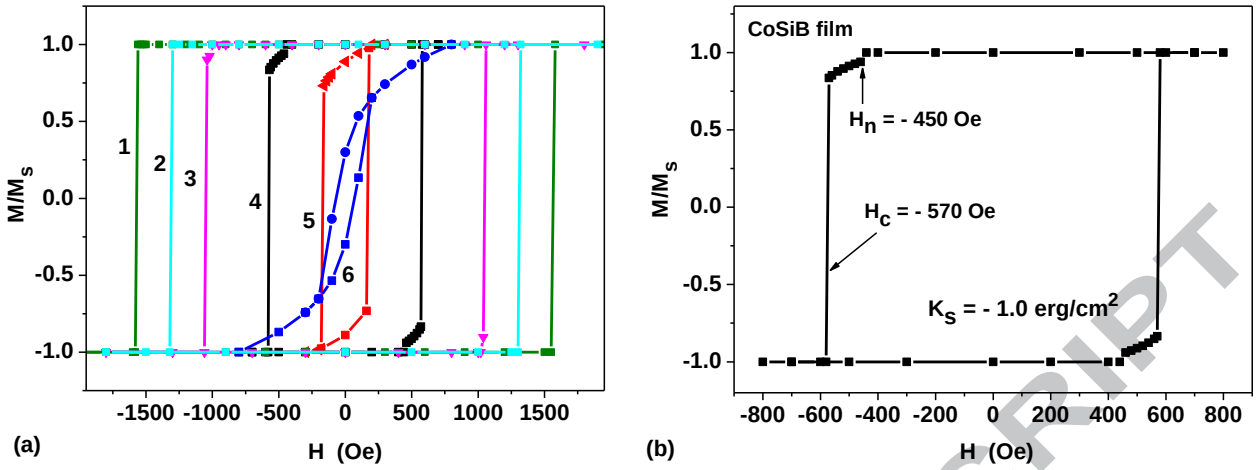

Fig. 3. a) Perpendicular hysteresis loops of rectangular CoSiB element with dimensions L_x = 360 nm, L_y = 120 nm, L_z = 6 nm, depending on the value of the surface anisotropy constant: 1) K_s = - 1.2 erg/cm^2; 2) K_s = - 1.15 erg/cm^2; 3) K_s = - 1.1 erg/cm^2; 4) K_s = - 1.0 erg/cm^2; 5) K_s = - 0.9 erg/cm^2; 6) K_s = - 0.8 erg/cm^2. b) Nucleation field and coercive force of the element with K_s = - 1.0 erg/cm^2.

Fig. 3a shows the perpendicular hysteresis loops of the rectangular thin-film element with aspect ratio L_x/L_y = 3.0, depending on the value of the surface anisotropy constant. With the numerical cell size b = 1.5 nm there are 240 numerical cells along the longest size of the element studied. As Fig. 3a shows, the coercive force of the perpendicular hysteresis loops of this element increases with increasing of $|K_s|$. For sufficiently large absolute values of $|K_s| \geq 1.15$ erg/cm^2 the hysteresis loops 1) and 2) in Fig. 3a are strictly rectangular. This means that for $|K_s| \geq 1.15$ erg/cm^2 the magnetization reversal process occurs in a strong negative magnetic field by a single Barkhausen jump. On the other hand, for $|K_s|$ in the interval $1.0 \leq |K_s| \leq 1.15$ erg/cm^2 (loops 3) and 4) in Fig. 3a), a nonlinear stabilization of the nucleation mode occurs in a certain range of magnetic fields just after the mode nucleation, where an intermediate non-uniform micromagnetic state exists. At the end of this interval the complete reversal of the element take place by single Barkhausen jump. Finally, for the values $|K_s| \leq 0.9$ erg/cm^2, the magnetization of the element is nonuniform even in zero magnetic field. Actually, it follows from an earlier analysis [16] that with a decrease in $|K_s|$ the perpendicularly magnetized z-state of the element transforms into the spin canted state. The hysteresis loops 5), 6) in Fig. 3a correspond to the spin canted micromagnetic state. For this state, in the absence of external magnetic field the average value of the unit magnetization vector is inclined at some angle to the surface of the element.

Fig. 3b shows in detail the magnetization reversal process of the same thin-film element with surface anisotropy constant K_s = - 1.0 erg/cm^2. For this element the nucleation field is given by H_n = - 450 Oe, whereas the Barkhausen jump that determines the coercive force of the element occurs in the field H_0 = -570 Oe. Consequently, a stable inhomogeneous micromagnetic state in this element exists within the interval $-570 < H_0 < -450$ Oe.

Fig. 4 shows the perpendicular hysteresis loops of a circular thin-film element with diameter D = 180 nm and thickness L_z = 6 nm, depending on the value of the surface anisotropy constant. The numerical cell size in these calculations is given by b = 1.5 nm. Thus, there are 120 numerical cells along the diameter of the element, so that its circular shape approximates with a reasonable accuracy. One can see that the behavior of the perpendicular hysteresis loops is similar to that of Fig. 3, but the numerical values of the nucleation fields for circular element differ from that of the rectangular sample. Similar results were also obtained for circular element of larger diameter, D = 240 nm.

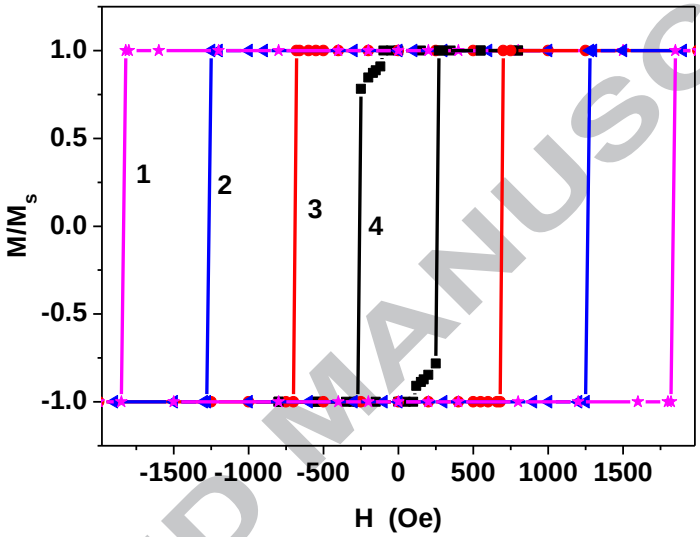

Fig. 4. Perpendicular hysteresis loops of a circular CoSiB element with diameter D = 180 nm and thickness L_z = 6 nm depending on the value of the surface anisotropy constant: 1) K_s = - 1.2 erg/cm^2; 2) K_s = - 1.1 erg/cm^2; 3) K_s = - 1.0 erg/cm^2; 4) K_s = - 0.9 erg/cm^2.

Nucleation mode

In general, the study of the nonlinear stabilization of the nucleation mode and the evaluation of the coercive force of the thin-film element can be performed only by numerical simulation. As an example, Fig. 5 shows successive steps 1) - 3) of the magnetization reversal process for rectangular and circular thin-film elements during the corresponding Barkhausen jumps. In Fig. 5 the areas where the α_z component of the unit magnetization vector is positive or negative are shown in red and in blue, respectively. Fig. 5a corresponds to the Barkhausen jump on curve 1) in Fig. 3a, whereas Fig. 5b show the evolution of the element magnetization during the Barkhausen jump on curve 3) in Fig. 4, correspondingly. As Fig. 5 shows, for both elements after the loss of stability of the homogeneous state the magnetization reversal proceeds owing to the formation and rapid propagation of the domain walls along the sample.

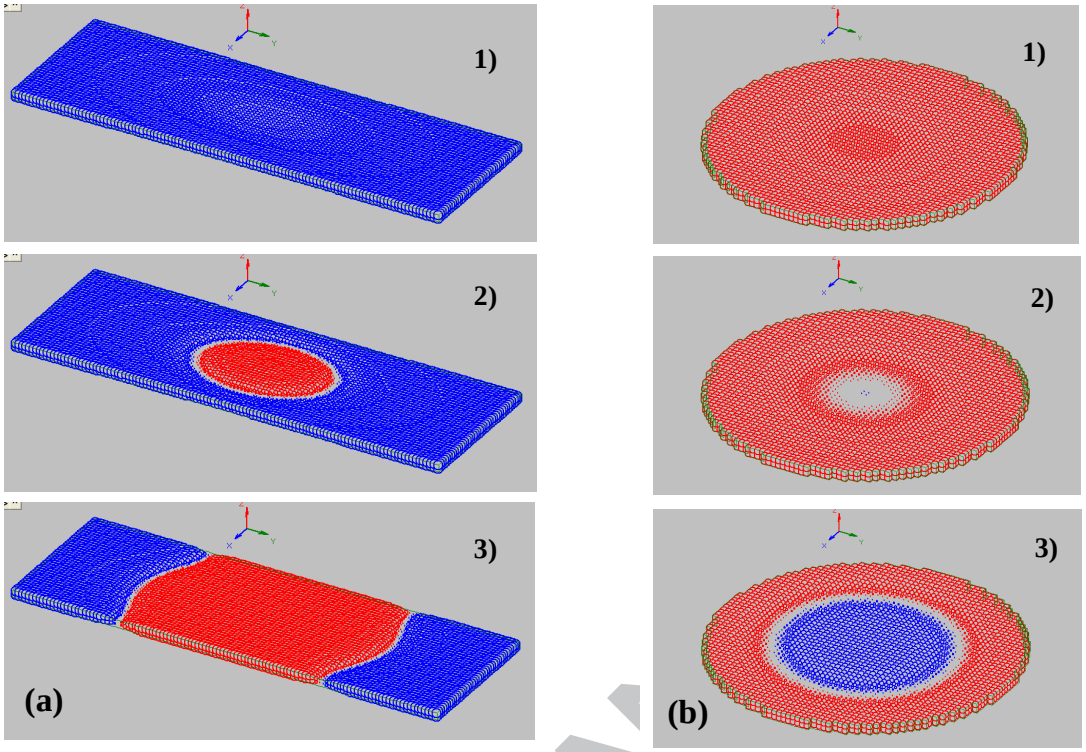

Fig. 5. Dynamics of magnetization reversal in thin-film elements: a) rectangular element with dimensions L_x = 360 nm, L_y = 120 nm, L_z = 6 nm and surface anisotropy constant K_s = -1.2 erg/cm^2 in magnetic field H_c = -1580 Oe; b) circular element with diameter D = 180 nm and thickness L_z = 6 nm, with a surface anisotropy constant K_s = - 1.0 erg/cm^2 at H_c = -700 Oe.

It is worth of mentioning that Fig. 5 shows only the late, nonlinear stage of magnetization reversal of the elements during the irreversible Barkhausen jumps. The latter occurs in a magnetic field corresponding to the coercive force of the element $H_0 = H_c$. At the same time, when the instability mode is just nucleated in the nucleation field, $H_0 = H_n$, the amplitude of the mode is very small. In this case the general nonlinear micromagnetic equations allow linearization [5]. The investigation of the nucleation fields of uniformly magnetized small ferromagnetic samples is one of the most important micromagnetic problems [5]. Unfortunately, the analytical investigation of the problem is possible [5] only for samples of high symmetry (sphere, long cylinder). Nevertheless, the value of the nucleation field and the shape of the corresponding lowest nucleation mode of the ferromagnetic element in the reversed magnetic field can be determined by means of numerical simulation.

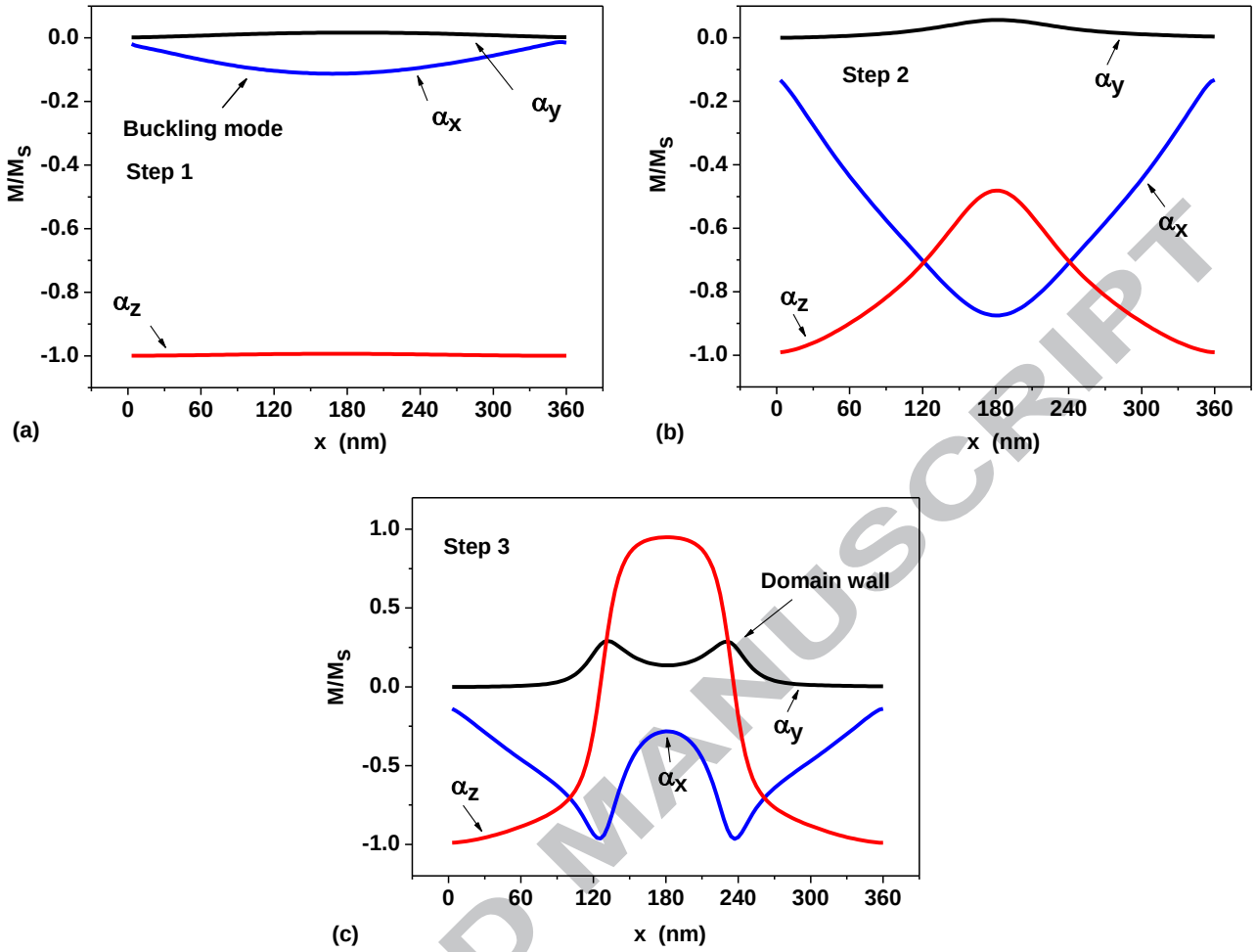

Fig. 6. The evolution of the magnetization distribution in the rectangular thin-film element with dimensions L_x = 360 nm, L_y = 120 nm, L_z = 6 nm and surface anisotropy constant K_s = -1.2 erg/cm^2 along the line $y = L_y/2$, $z = L_z$ during magnetization reversal in applied magnetic field H_c = -1580 Oe: a) the shape of the buckling nucleation mode at the initial stage of the process, b), c) the transient inhomogeneous magnetization distributions at the subsequent stages of the process.

Fig. 6a shows the shape of the nucleation mode for the rectangular element with dimensions L_x = 360 nm, L_y = 120 nm, L_z = 6 nm and surface anisotropy constant K_s = -1.2 erg/cm^2 at the initial stage of the magnetization reversal process in the magnetic field H_c = -1580 Oe. The magnetization distribution shown in Fig. 6a corresponds to the well known buckling mode, which exists in elongated small ferromagnetic samples [5]. The numerical cell size in the calculation of the buckling mode equals b = 1.5 nm. For the rectangular element with the aspect ratio L_x/L_y = 3.0, the buckling nucleation mode can be approximated with a good accuracy by the equations

$$\alpha_x = A\sin(\pi x/L_x); \qquad \alpha_y = 0.0; \qquad \alpha_z = \pm\sqrt{1-\alpha_x^2-\alpha_y^2}, \tag{8}$$

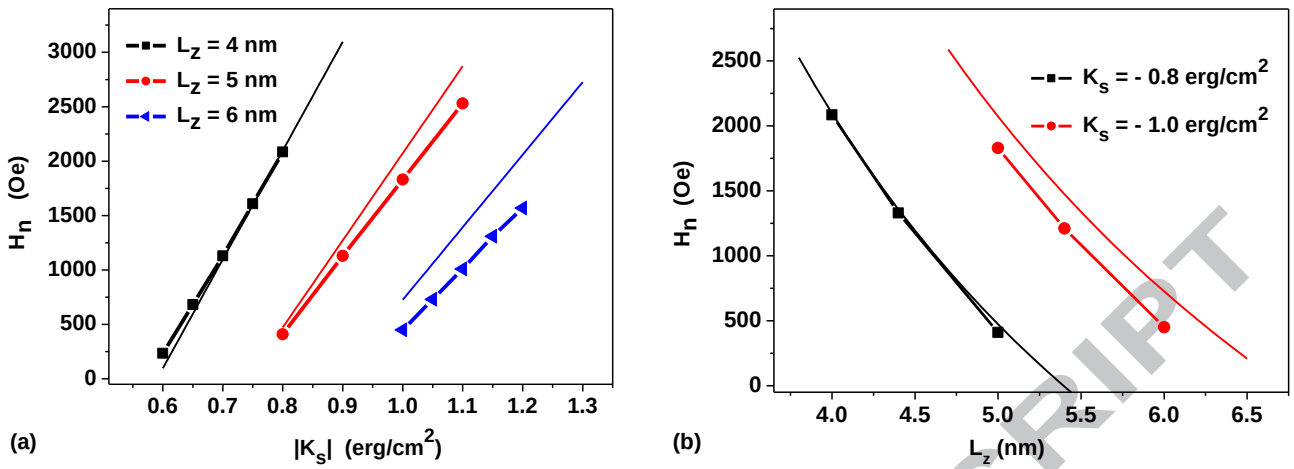

Fig. 7. The nucleation field of the buckling mode in rectangular samples with the aspect ratio L_x/L_y = 3.0: a) as a function of $|K_s|$ for different film thickness L_z; b) as a function of L_z for fixed values of the surface anisotropy constant. The solid lines are drawn according to Eq. (12).

where A is the mode amplitude, small at the initial stage of the reversal. Fig. 6b, 6c show the nonlinear evolution of the buckling mode at the late stages of the development of this instability (see also Fig. 5a).

Figs. 7a, 7b show calculated numerically (dots) the dependence of the nucleation field of rectangular thin-film elements with aspect ratio L_x/L_y = 3.0 on the value of the surface anisotropy constant, and on the thickness of the element, respectively. For thickness L_z = 6 nm the in-plane dimensions of the element are given by L_x = 360 nm, L_y = 120 nm, the numerical cell size being b = 1.5 nm. For smaller thickness the in-plane dimensions and numerical cell size are scaled accordingly. Since the shape of the nucleation mode for this element is known (see Eq. (8)), the value of the corresponding nucleation field can be approximately determined by means of a variational estimate [5].

The second order correction to the total energy of the z-state of the rectangular element due to the magnetization perturbation of the first, $\vec{\alpha}^{(1)} = (\alpha_x, 0, 0)$, and the second, $\vec{\alpha}^{(2)} = (0, 0, -\alpha_x^2/2)$, orders of magnitude has the form

$$\delta W^{(2)} = \frac{C}{2}\int dv\left(\vec{\nabla}\alpha_x\right)^2 + |K_s|\int ds\,\alpha_x^2 - \left(\frac{M_s\left(H_0 + \left|H_z'^{(0)}\right|\right)}{2} + K_V\right)\int dv\,\alpha_x^2 + \frac{1}{8\pi}\int dv\left(\vec{H}'^{(1)}\right)^2 . \quad (9)$$

Here the first term gives the perturbation of the exchange energy of the element, the second term, where the integral is taken over the element surface, $z = L_z$, gives the perturbation of the surface anisotropy energy, the third term is the Zeeman energy perturbation, the perturbation of the volume magnetic anisotropy, and part of the magnetostatic energy perturbation. The unperturbed

demagnetizing field of the element can be expressed through the demagnetizing factor of the sample, $H_z'^{(0)} = -N_z M_s$. Finally, the last term in Eq. (9) is the magnetostatic energy associated with the first-order magnetization perturbation, $\vec{\alpha}^{(1)}$. Due to the small thickness of the element, the main contribution to this energy is the self magnetostatic energy of the volume magnetic charges $\rho(x)$,

$$\delta W_m^{(2)} = \frac{1}{8\pi}\int dv\left(\vec{H}'^{(1)}\right)^2 = \frac{1}{2}\int dv dv_1 \frac{\rho(x)\rho(x_1)}{\left|\vec{r}-\vec{r}_1\right|}, \tag{10a}$$

distributed in the volume of the element with the density

$$\rho(x) = -M_s \frac{d\alpha_x}{dx} = -AM_s \frac{\pi}{L_x}\cos\left(\frac{\pi x}{L_x}\right). \tag{10b}$$

Taking into account the small thickness of the element, the magnetostatic energy, Eq. (10), can be evaluated as follows

$$\delta W_m^{(2)} = \frac{(\pi M_s A)^2}{2} V \frac{L_z}{L_x} Q\left(\frac{L_x}{L_y}\right), \tag{11}$$

where $V = L_x L_y L_z$ is the volume of the element, the dimensionless function $Q(\xi)$ being

$$Q(\xi) = \int_0^1 dx \int_0^1 dx_1 \int_0^1 dy \cos(\pi x)\cos(\pi x_1)\ln\frac{1+y+\sqrt{\xi^2(x-x_1)^2+(1+y)^2}}{y+\sqrt{\xi^2(x-x_1)^2+y^2}}.$$

The maximum value of this function calculated numerically is given by $Q_{\max} \approx 0.12$ at $\xi = 5.4$. Then it decreases as the function of parameter ξ, $Q \sim 1/\xi$.

Equating the total energy correction, Eq. (9) to zero, one obtains the nucleation field of the buckling mode of the rectangular thin-film element as

$$H_n = \frac{C}{M_s}\left(\frac{\pi}{L_x}\right)^2 + \frac{2|K_s|}{M_s L_z} - \left|H_z'^{(0)}\right| - \frac{2K_V}{M_s} + 2\pi^2 M_s \frac{L_z}{L_x} Q\left(\frac{L_x}{L_y}\right). \tag{12}$$

For sufficiently large in-plane dimensions of the element, L_x, $L_y >> L_z$, the main contributions to this expression are given by the second term, which describes the effect of surface anisotropy, and the third term, which gives a large demagnetizing field of the element magnetized perpendicular to the plane, $\left|H_z'^{(0)}\right| \approx 4\pi M_s$. For example, for the thin film element with dimensions L_x = 240 nm, L_y = 80 nm, L_z = 4 nm and surface anisotropy constant K_s = -0.6 erg/cm^2 the values of the successive terms in Eq. (12) are given by 68.5, 6000, - 5950, -40, and 19.5 Oe, respectively.

Since the demagnetizing field of a thin-film element is only slightly depended on its thickness in the range of small thickness L_z = 4 - 6 nm, the nucleation field of the buckling mode turns out to be proportional to the absolute value of the surface anisotropy constant $|K_s|$, and inversely proportional to

the thickness of the element L_z. The solid lines in Fig. 7 are drawn in accordance with Eq. (12). As Fig. 7 shows, the variation estimate of the nucleation field, Eq. (12), is in a qualitative agreement with the numerical calculations of the nucleation fields of rectangular thin-film elements with surface anisotropy.

Conclusion

In this paper the magnetization reversal process in thin-film ferromagnetic elements with surface anisotropy of various shapes and sizes is investigated. The dependence of the perpendicular and in-plane hysteresis loops on the element thickness, and the value of the surface anisotropy constant is studied. It is shown that for sufficiently large values of the surface anisotropy constant, the magnetization reversal in elongated thin-film elements is due to nucleation of the buckling mode. For the rectangular element the approximate formula is obtained for the dependence of the nucleation field of the buckling mode on the element thickness and the magnitude of the surface anisotropy constant. The numerical results obtained turn out to be in reasonable agreement with approximate analytical calculations of the slope of the element magnetization curve in a small in-plane magnetic field, as well as the nucleation field of the buckling mode in magnetic field perpendicular to the element plane.

The investigation of the magnetization reversal process in thin-film elements with surface anisotropy is important for better understanding of magnetic properties of such elements having vital applications in modern thin-film electronics devices. It enables one also to carry out accurate determination of the surface anisotropy constant K_s from the experiment.

Acknowledgement

The authors wish to acknowledge the financial support of the Ministry of Education and Science of the Russian Federation in the framework of Increase Competitiveness Program of NUST «MISIS», contract № K2-2015-018.

References

[1] Q.L. Ma, S. Iihama, T. Kubota, X.M. Zhang, S. Mizukami, Y. Ando, T. Miyazaki, Appl. Phys. Lett. 101 (2012) 122414.

[2] J. Yoon, S. Jung, Y. Choi, J. Cho, C.-Y. You, M.H. Jung, H.I. Yim, J. Appl. Phys. 113 (2013) 17A342.

[3] S. Mangin, D. Ravelosona, J.A. Katine, M.J. Carey, B.D. Terris, E.E. Fullerton, Nature Mater. 5 (2006) 210.

[4] C.-H. Lambert, A. Rajanikanth, T. Hauet, S. Mangin, E.E. Fullerton, S. Andrieu, Appl. Phys. Lett. 102 (2013) 122410.

[5] W.F. Brown, Jr., *Micromagnetics* (Wiley-Interscience, New York - London, 1963).

[6] M.T. Johnson, P.J.H. Bloemen, F.J.A. den Broeder, J.J. de Vries, Rep. Prog. Phys. 59 (1996) 1409.

[7] H.N. Bertram, D.I. Paul, J. Appl. Phys. 82 (1997) 2439.

[8] C.A.F. Vaz, J.A.C. Bland, G. Lauhoff, Rep. Prog. Phys. 71 (2008) 056501.

[9] R. Allenspach, M. Stampanoni, A. Bischof, Phys. Rev. Lett. 65 (1990) 3344.

[10] H. Fritzsche, J. Kohlepp, H.J. Elmers, U. Gradmann, Phys. Rev. B 49 (1994) 15665.

[11] M. Speckmann, H. P. Oepen, H. Ibach, Phys. Rev. Lett. 75 (1995) 2035.

[12] M. Hehn, S. Padovani, K. Ounadjela, and J. P. Bucher, Phys. Rev. B 54 Σ1996Π 3428.

[13] H.X. Yang, M. Chshiev, B. Dieny, J.H. Lee, A. Manchon, K.H. Shin, Phys. Rev. B 84 (2011) 054401.

[14] K.H. He, S.J. Chen, J. Appl. Phys. 111 (2012) 07C109.

[15] J.I. Hong, S. Sankar, A.E. Berkowitz, W.F. Egelhoff Jr., J. Magn. Magn. Mater. 285 (2005) 359.

[16] N.A. Usov, O.N. Serebryakova, J. Appl. Phys. 121 (2017) 133905.